



ELSEVIER

Available online at www.sciencedirect.com

SCIENCE @ DIRECT®

Journal of Sound and Vibration 280 (2005) 531–553

JOURNAL OF
SOUND AND
VIBRATION

www.elsevier.com/locate/jsvi

Evaluation of different methods for the consideration of the effect of rotation on the stiffening of rotating beams

A.A. Al-Qaisia*, B.O. Al-Bedoor¹

Mechanical Engineering Department, Faculty of Engineering and Technology, University of Jordan, Amman 11942, Jordan

Received 14 October 2003; accepted 9 December 2003

Available online 29 September 2004

Abstract

This paper addresses the problem of the rotating beam axial shortening modelling. The different methods for accounting for the rotating beam axial shortening are used to develop four different models. The models are named as the potential energy model (PM), kinetic energy model (KM), and kinetic and potential energy model (KPM), in addition to the model that does not account for the axial shortening named as the consistent model (CM). The PM model accounts for the axial shortening in the form of added elastic potential energy that results from the virtual work done by the centrifugal force. In the KM model, the shortening effect is included in the velocity vector and the corresponding kinetic energy. Finally the KPM model combines both approaches. The results of analysis showed that the approach which handles both the effect of rotating speed and the effect of vibration amplitude for all modes correctly is the PM model. The KM model reflected softening behaviour that cannot be accepted physically by rotating structures for higher modes. Moreover, the combined KPM method showed in-correctness at low amplitudes that contradicts the linear theory.

© 2004 Elsevier Ltd. All rights reserved.

*Corresponding author. Fax.: +962-6-535-5588.

E-mail address: alqaisia@ju.edu.jo (A.A. Al-Qaisia).

¹On leave from King Fahd University of Petroleum and Minerals, Dhahran, Saudi Arabia

1. Introduction

The issue of developing accurate dynamic models of rotating flexible structures has attracted the attention of many researchers and design engineers due to the growing need to operate and control rotating flexible members with well-predicted dynamic behaviour. Consistent mathematical models that addressed the beam as the typical rotating element and considered only the beam transverse deflection have resulted in softening effect that allowed rotating beams to a critical speed after which the beam became statically unstable. This behaviour contradicts the practical physics of the problem that forced researchers to seek techniques to compensate for this contradiction through studying the associated stiffening effect produced by the centrifugal forces. These centrifugal forces can be imposed in the dynamic model by a correction action through adding potential energy that is produced by material centrifugal forces in conjunction with the axial shortening due to beam transverse deflection. Alternatively other researchers imposed the geometrical condition known as the inextensibility condition into the generic material point position vector that leads automatically to the inclusion of shortening effect in the system kinetic energy. The previous two approaches of correcting for the shortening effect have been used by different research studies in calculating the rotating beam natural frequencies and some studies on the dynamic response simulation. Few studies were reported that addressed the effect of the approach on the resulting system natural frequencies and dynamic response. However, the reported analysis results were limited and no quantified assessment was reached. This work is motivated to put together analysis results and discussions and to put quantified assessment on the aspects related to the effects on natural frequencies, dynamic simulation and nonlinear analysis.

Hoa [1] studied the natural frequencies of a rotating beam with tip mass. The stiffening effect was included in the formulation by substituting the resulted stress created by centrifugal forces into the bending strain energy. Kane et al. [2] studied the dynamics of a cantilever beam attached to a moving base. The beam axial extension is included into the elastic degrees of freedom, but results were reported for the rigid body motions “translation and rotation”. Baruh and Tadikonda [3] reported issues on the dynamics and control of flexible robot manipulators. The axial shortening due to bending deflection was substituted in the kinetic energy expressions. They observed that if the flexibility is included the resulting angular velocity will be higher and the angular position is deviated from the target position. Lee [4] studied the vibration of an inclined rotating cantilever beam with tip mass. The work done by the centrifugal forces was substituted in the potential energy. Results were presented for the effect of rotational speed, tip mass and inclination angle on the natural frequencies. Mulmule et al. [5] used the same approach in Ref. [4] to study the flexural vibration of rotating tapered Timoshenko beam attached to a rigid hub with setting angle. Tadikonda and Chang [6] accounted for the axial shortening through the potential energy contribution from the centrifugal force. Al-Bedoor [7,8] studied dynamic response of coupled shaft torsional and blade bending vibrations. The effect of axial shortening was considered in the formulation by substituting the work done by the centrifugal force in the potential energy expression. Al-Bedoor and Hamdan [9] studied the nonlinear dynamic behaviour of a rotating flexible arm. The axial shortening due to bending deformation was included in the kinetic energy expressions. Deviations in the target position were faced for certain arm lengths and properties. Al-Qaisia [10,11] used the same approach in Ref. [9] to study the non-linear natural frequencies and the dynamic behaviour of a rotating cantilever beam attached to a rigid hub with an angle and carrying inertia element.

When it comes to investigating the effect of the method for accounting for the axial shortening on the obtained results only El-Absy et al. [12] can be found. They studied the effect of geometric stiffness forces on the stability of elastic and rigid body modes. They presented three approaches in modelling the rotating beam; (1) consistent complete model (CCM), in which the effect of axial shortening due to bending deformation is included in both the inertia and elastic forces; (2) consistent incomplete model (CIM), the axial shortening is neglected in both the inertia and elastic forces; (3) second inconsistent model (SIM), the axial shortening is included in inertia forces and neglected in elastic forces formulations. Results were presented for the three models and they concluded that the three models lead to stable solutions at high values of angular velocities and the inclusion of the effect of axial shortening in the inertia forces is not the only approach that can be used to maintain stability at high angular velocities. However, they depended on only investigating the dynamic response and no results were presented either for the natural frequencies or for the effect of amplitude of vibration.

In this study a unified mathematical model that allows use of the potential energy approach and the inextensibility condition in the mathematical model of the rotating flexible beam is presented. The model without any correction is used as the base model for comparison purposes. The important parameters are identified and the natural frequencies and fast Fourier transform (FFT) of the system response are studied for comparison. Finally, the three models' frequency responses are studied using the method of harmonic balance for evaluation and investigating the effect of large amplitude of vibration.

2. The mathematical models

2.1. Consistent model (CM)

The global position vector of an arbitrary point P , in the XY inertial coordinates, Fig. 1, on the beam can be written as

$$R_P = R_H + [A(\theta)]r_P, \quad (1)$$

where r_P is the position vector of the point P in the rotating body coordinate system xy , $A[(\theta)]$ is the rotational transformation matrix from the body coordinate xy system to the inertial coordinates XY and R_H is the position vector of the origin of the rotating body coordinate system xy in the inertial coordinate XY .

To develop the kinetic energy expression the velocity vector \dot{R}_P can be represented as follows:

$$\dot{R}_P = \dot{R}_H + [A(\theta)]\dot{r}_P + \dot{\theta}[A_\theta(\theta)]r_P \quad (2)$$

where $A_\theta(\theta) = [dA/d\theta]$, $\dot{R}_H = \dot{\theta}R_H(-\sin \theta \hat{i} + \cos \theta \hat{j})$, $r_P = si + vj$ and $\dot{r}_P = \dot{u}\hat{i} + \dot{v}\hat{j}$.

Upon substituting for \dot{R}_H , r_P , \dot{r}_P , $[A(\theta)]$ and $[A_\theta(\theta)]$ into Eq. (2), the velocity vector \dot{R}_P in the inertial coordinate system XY can be expressed as

$$\dot{R}_P = \left\{ \begin{array}{l} -\alpha \sin \theta + \gamma \cos \theta \\ \alpha \cos \theta + \gamma \sin \theta \end{array} \right\}, \quad (3)$$

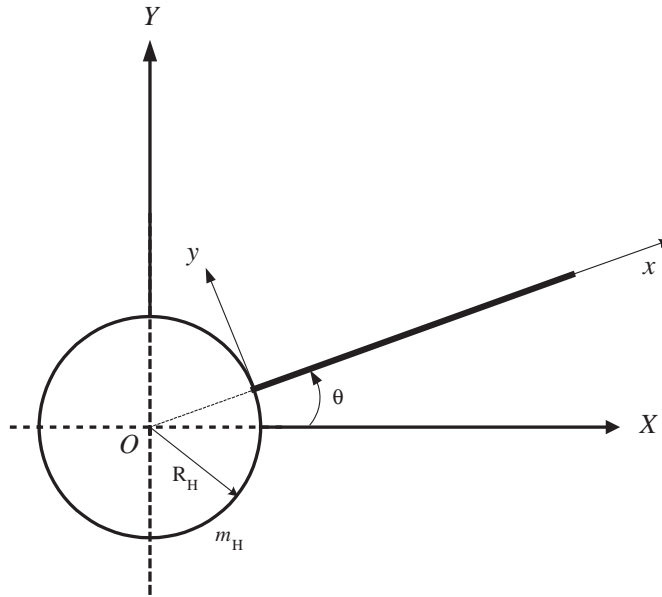


Fig. 1. A schematic of the rotating beam–hub system.

where

$$\alpha = \dot{\theta}(R_H + s) + \dot{v},$$

$$\gamma = -\dot{\theta}v.$$

Now, the kinetic energy of the beam–mass–hub system under consideration can be expressed as

$$KE = \frac{1}{2}m_b \int_0^1 \dot{R}_P^T \cdot \dot{R}_P d\zeta + \frac{1}{2}I_H \dot{\theta}^2, \tag{4}$$

where $m_b = \rho l$ is the constant mass of the beam, $\zeta = s/l$ is dimensionless position of the material point, I_H is the mass moment of inertia of the hub ($I_H = m_H R_H^2/2$) and m_H is the mass of the hub.

Substituting Eq. (3) into Eq. (4), the kinetic energy of the considered system takes the form

$$KE = \frac{1}{2}m_b \int_0^1 \{ \dot{\theta}^2 [(s + R_H)^2 + v^2] + 2\dot{\theta}[\dot{v}(s + R_H)] + \dot{v}^2 \} d\zeta + \frac{1}{2}I_H \dot{\theta}^2. \tag{5}$$

The beam elastic potential energy with flexural rigidity EI is given by

$$PE = \frac{EI\lambda^3}{2} \int_0^1 v''^2 d\zeta, \tag{6}$$

where $\lambda = 1/l$. Using Eqs. (5) and (6) for the kinetic and potential energy expressions, respectively, the Lagrangian of the system L can be obtained, which upon discretizing us the

assumed mode method

$$v(\zeta, t) = \sum_{i=1}^N \phi_i(\zeta)q_i(t) \tag{7}$$

takes the form

$$L = \frac{m_B l^2}{2} \{ \beta_1 \dot{\theta}^2 + \beta_2 \dot{\theta}^2 q^2 + \beta_3 \dot{\theta} \dot{q} + \beta_4 \dot{q}^2 - \beta^2 \beta_5 q^2 \}, \tag{8}$$

where $\phi_i(\zeta)$ is the normalized, self-similar (i.e. independent of the motion amplitude) assumed mode shape of the cantilever beam, $q_i(t)$ is an unknown time-dependent generalized coordinate and N is the number of modes.

Applying Lagrange’s equations, the system equations of motion can be written as

$$2[\beta_1 + \beta_2 q^2] \ddot{\theta} + 4\beta_2 q \dot{q} \dot{\theta} + \beta_3 \ddot{q} = \frac{2T}{m_B l^2}, \tag{9}$$

$$2\beta_4 \ddot{q} + 2[\beta^2 \beta_5 - \beta_2 \dot{\theta}^2] q + \beta_3 \ddot{\theta} = 0, \tag{10}$$

where the different coefficients are defined as follows:

$$\begin{aligned} \beta^2 &= \frac{EI \lambda^4}{\rho} \\ \beta_1 &= a_1 + \frac{1}{3} + \frac{R_H}{l} + \left(\frac{R_H}{l}\right)^2 a_1 = \frac{m_H}{m_b}, \\ \beta_2 &= \int_0^1 \phi^2 d\zeta, \\ \beta_3 &= 2 \int_0^1 \phi \left(\zeta + \frac{R_H}{l}\right) d\zeta, \\ \beta_4 &= \int_0^1 \phi^2 d\zeta, \\ \beta_5 &= \int_0^1 \phi''^2 d\zeta. \end{aligned} \tag{11}$$

Looking into Eqs. (9) and (10), one can find that the model consists of two coupled ordinary differential equations. One of the equations represents rigid body motion and the second represents the elastic deflection of the beam. Moreover, one can observe that Eq. (10) yields static instability if the coefficient of q goes to zero which can occur if the system is rotated to a certain angular velocity $\dot{\theta}$ which is equal to the beam natural frequency. This behaviour is practically not true as rotating beams get stiffened as a result of rotation. To compensate for this behaviour the effect of shortening was included in previous studies [7–12].

2.2. Beam axial shortening due to bending deformations

If the beam deformed position is considered it was observed that the axial position of the material point changes as can be seen in Fig. 2. Geometrically one can relate the axial shortening to the transverse deflection. Before deformation the position of a point on the elastic axis is given by $r_0 = si$. After deformation, its position is given by $r = (s - u)i + vj$, where i , and j are the unit vectors before and after deformation. Hence, the strain e along the elastic axis of a differential element is defined by [13]

$$e = \left(\frac{\partial r}{\partial s} \bullet \frac{\partial r}{\partial s} \right)^{1/2} - \left(\frac{\partial r_0}{\partial s} \bullet \frac{\partial r_0}{\partial s} \right)^{1/2} = \sqrt{(1 - \lambda u')^2 + (\lambda v')^2} - 1, \tag{12}$$

where $\lambda = 1/l$ and primes are derivatives with respect to the dimensionless arc length ζ . For inextensional beams, the elongation e is assumed to be zero, resulting in the condition [13],

$$(1 - \lambda u')^2 + (\lambda v')^2 = 1 \tag{13}$$

The inextensibility condition (13), allows one to relate, through a consistent geometric consideration, the axial and the lateral displacement. Eq. (13) may be written as $(1 - \lambda u') = \sqrt{1 - (\lambda v')^2}$. Noting that $(\lambda v')^2 \ll 1$, expanding the right-hand side into a power series, retaining nonlinear terms up to the second order, and integrating the result from 0 to an arbitrary value of ζ leads to the following expression for the axial displacement (shortening) u due to the flexural bending v ;

$$u = \frac{1}{2} \int_0^\zeta \left(\lambda v'^2 + \frac{\lambda^3}{4} v'^4 \right) d\zeta. \tag{14}$$

Eq. (14) is the relation between the axial position of the material point u and the beam transverse deflection v . Previous researchers have used this expression to model the added energy to the system either (1) in the potential energy using the virtual work that is produced by this

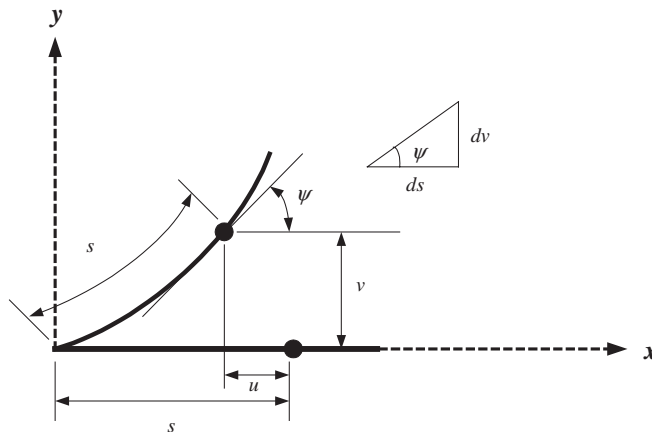


Fig. 2. The deformed inextensible beam.

displacement and the centrifugal force due to rotation or (2) in the kinetic energy by accounting for the axial position as time-dependent variable. Moreover, one possibility is to add both the effects as they seem not to violate each other. In the following sections, the equations of motion are derived by using each of the three approaches.

2.3. Potential energy model (PM)

The system potential energy is constituted from the elastic beam strain energy V_E and the potential energy of the axial shortening due to transverse deformation and the motion generated inertial force, V_A . The elastic beam nonlinear strain energy for the beam is given by

$$V_E = \frac{EI\lambda^3}{2} \int_0^1 (v''^2 + \lambda^2 v'' v'^2) d\zeta. \tag{15}$$

The inertial force on the material point P of the beam results from the rotational motion can be expressed in the form

$$F_P = \int_{\zeta}^1 \rho(R_H + l\zeta)\dot{\theta}^2 l d\zeta = \rho l^2 \dot{\theta}^2 \int_{\zeta}^1 \left(\frac{R_H}{l} + \zeta \right) d\zeta. \tag{16}$$

Upon evaluating the integral given in Eq. (16), the inertial force is given by

$$F_P = \rho l^2 \dot{\theta}^2 \left[\frac{R_H}{l} (1 - \zeta) + \frac{1}{2} (1 - \zeta^2) \right]. \tag{17}$$

The virtual work that results from the axial shortening u under the effect of the inertial forces of Eq. (23) can be called the axial shortening potential energy and can be written as

$$V_A = \int_0^1 F_P \cdot du. \tag{18}$$

Substituting the inertial force (16) and the axial shortening (14) into the integral of Eq. (18) yields

$$V_A = \frac{-\rho l^2 \dot{\theta}^2}{2\lambda} \int_0^1 \left\{ \frac{R_H}{l} (1 - \zeta) + \frac{1}{2} (1 - \zeta^2) \right\} \left(\lambda^2 v'^2 + \frac{\lambda^4}{4} v'^4 \right) d\zeta. \tag{19}$$

Evaluating the integral and substituting $v(\zeta, t) = \phi q / \lambda$, the axial shortening potential energy can be expressed as

$$V_A = \frac{-\rho l^2 \dot{\theta}^2}{2\lambda} \int_0^1 \left\{ \frac{R_H}{l} (1 - \zeta) + \frac{1}{2} (1 - \zeta^2) \right\} \left(q^2 \phi'^2 + \frac{1}{4} q^4 \phi'^4 \right) d\zeta. \tag{20}$$

Now the system potential energy becomes

$$PE = V_A + V_E. \tag{21}$$

The system kinetic energy can be obtained by using the same procedure followed in the previously. Accordingly the system kinetic energy is given by

$$\begin{aligned} \text{KE} = & \frac{1}{2}m_b \int_0^1 (\dot{\theta}^2[(s + R_H)^2 + v^2] \\ & + 2\dot{\theta}[\dot{v}(s + R_H)] + \dot{v}^2)d\zeta + \frac{1}{2}I_H\dot{\theta}^2. \end{aligned} \quad (22)$$

Using the expression of the kinetic and potential energies of the beam-hub system, the Lagrangian, $L = \text{KE} - \text{PE}$, can be written in the form:

$$\begin{aligned} L = & \frac{m_B l^2}{2} \{ \beta_1 \dot{\theta}^2 + \beta_2 \dot{\theta}^2 q^2 + \beta_3 \dot{\theta} \dot{q} + \beta_4 \dot{q}^2 - \beta^2 \beta_5 q^2 \\ & - \beta^2 \beta_6 q^4 - \beta_7 \dot{\theta}^2 q^2 - \beta_8 \dot{\theta}^2 q^4 \}, \end{aligned} \quad (23)$$

where the inclusion of the added potential energy in the Lagrangian produced the following added terms:

$$\begin{aligned} \beta_6 = & \int_0^1 \phi'^2 \phi''^2 d\zeta \\ \beta_7 = & - \int_0^1 \phi'^2 \left(\frac{R_H}{l} + \frac{1}{2} - \zeta - \frac{\zeta^2}{2} \right) d\zeta \\ \beta_8 = & \frac{-1}{4} \int_0^1 \phi'^4 \left(\frac{R_H}{l} + \frac{1}{2} - \zeta - \frac{\zeta^2}{2} \right) d\zeta \end{aligned} \quad (24)$$

Using the virtual work method and the system Lagrangian Eq. (23), the system equations of motion are obtained for θ and q , as follows:

$$2[\beta_1 + (\beta_2 - \beta_7)q^2 - \beta_8 q^4]\ddot{\theta} + 4(\beta_2 - \beta_7)\dot{\theta}q\dot{q} - 8\beta_8\dot{\theta}q^3\dot{q} + \beta_3\ddot{q} = \frac{2T}{m_B l^2}, \quad (25)$$

$$2\beta_4\ddot{q} + 2[\beta^2\beta_5 + (\beta_7 - \beta_2)\dot{\theta}^2]q + 4[\beta^2\beta_6 + \beta_8\dot{\theta}^2]q^3 + \beta_3\ddot{\theta} = 0. \quad (26)$$

Eqs. (25) and (26) are similar to Eqs. (9) and (10), except for added terms which are shown to stiffen the beam as a function of angular velocity, in addition to an extra cubic nonlinear term that also has its coefficient as function of the rotating speed.

2.4. The kinetic energy model (KM)

Following the same procedure as in Section 2.1, the kinetic energy is developed. The difference is in the description of the material position vector $r_p = (s - u)i + vj$ in the body coordinate system that considers the axial shortening. Where s is the undeflected position, $u(s, t)$ is the axial shortening due to bending deformation and $v(s, t)$ is the transverse deflection of the material point P measured with respect to the hub coordinate system xy , i and j are the unit vectors along x and y , respectively, (Fig. 2). As a result the velocity vector of the material point in the inertial reference

frame can be expressed as

$$\dot{R}_P = \left\{ \begin{array}{l} -\alpha \sin \theta + \beta \cos \theta \\ \alpha \cos \theta + \beta \sin \theta \end{array} \right\}, \tag{27}$$

where

$$\alpha = \dot{\theta}(R_H + (s - u)) + \dot{v},$$

$$\beta = -(\dot{\theta}v + \dot{u})$$

the kinetic energy of the system takes the form

$$\text{KE} = \frac{1}{2}m_b \int_0^1 \left(\dot{\theta}^2 [(s - u) + R_H]^2 + v^2 \right) d\zeta + 2\dot{\theta}[\dot{v}(s - u) + R_H] + \dot{v}^2 + \dot{u}^2 \tag{28}$$

Note that the system kinetic energy in Eq. (28) is a function of the velocity variables \dot{u} , \dot{v} , angular velocity $\dot{\theta}$. The axial velocity \dot{u} can be eliminated from the system kinetic energy expression by substituting Eq. (14).

Upon substituting Eq. (28), and the previous expression for the elastic potential the Lagrangian expression can be written as

$$L = \frac{m_B l^2}{2} \left\{ \begin{array}{l} \beta_1 \dot{\theta}^2 + \beta_2 \dot{\theta}^2 q^2 + \beta_3 \dot{\theta} \dot{q} + \beta_4 \dot{q}^2 - \beta^2 \beta_5 q^2 - \beta^2 \beta_6 q^4 \\ -\beta_9 \dot{\theta}^2 q^2 + \beta_{10} \dot{\theta}^2 q^4 - \beta_{11} \dot{\theta}^2 q^4 + \beta_{12} \dot{\theta} \dot{q} q^2 + \beta_{13} q^2 \dot{q}^2 \end{array} \right\}, \tag{29}$$

where the added terms due to the inclusion of the inextensibility condition have the following coefficients

$$\beta_9 = \int_0^1 \zeta \left(\int_0^\zeta \phi'^2 d\chi \right) d\zeta + \frac{R_H}{l} \int_0^1 \left(\int_0^\zeta \phi'^2 d\chi \right) d\zeta,$$

$$\beta_{10} = \frac{1}{4} \left[\int_0^1 \left(\int_0^\zeta \phi'^2 d\chi \right)^2 d\zeta \right],$$

$$\beta_{11} = \frac{1}{4} \int_0^1 \zeta \left(\int_0^\zeta \phi'^4 d\chi \right) d\zeta + \frac{R_H}{4l} \int_0^1 \left(\int_0^\zeta \phi'^4 d\chi \right) d\zeta, \tag{30}$$

$$\beta_{12} = \int_0^1 \phi \left(\int_0^\zeta \phi'^2 d\chi \right) d\zeta,$$

$$\beta_{13} = \int_0^1 \left(\int_0^\zeta \phi'^2 d\chi \right)^2 d\zeta.$$

By applying Lagrange’s equation to the system Lagrangian equation (29), the system equations of motion are obtained as

$$2[\beta_1 + (\beta_2 - \beta_9)q^2 + (\beta_{10} - \beta_{11})q^4]\ddot{\theta} + 4(\beta_2 - \beta_9)\dot{\theta}q\dot{q} + 8(\beta_{10} - \beta_{11})\dot{\theta}q^3\dot{q} + \beta_3\ddot{q} + \beta_{12}(\ddot{q}q^2 + 2\dot{q}^2q) + \frac{2T}{m_B l^2} = 0 \tag{31}$$

$$2[\beta_4 + \beta_{13}q^2]\ddot{q} + [\beta_3 + \beta_{12}q^2]\ddot{\theta} + 2[\beta^2\beta_5 - (\beta_2 - \beta_9)\dot{\theta}^2]q + 4[\beta^2\beta_6 - \beta_{10}\dot{\theta}^2 + \beta_{11}\dot{\theta}^2]q^3 + 2\beta_{13}q\dot{q}^2 = 0. \tag{32}$$

Eqs. (31) and (32) represent the same problem of coupled rigid body and beam generalized deflection as Eqs. (9) and (10) and Eqs. (25) and (26).

2.5. Kinetic and potential model (KPM)

Here in this section the axial shortening is substituted into the kinteic and potential expressions. Wherein, the Lagrangian of the system becomes

$$L = \frac{m_B l^2}{2} \left\{ \begin{array}{l} \beta_1 \dot{\theta}^2 + \beta_2 \dot{\theta}^2 q^2 + \beta_3 \dot{\theta} \dot{q} + \beta_4 \dot{q}^2 - \beta^2 \beta_5 q^2 - \beta^2 \beta_6 q^4 - \beta_7 \dot{\theta}^2 q^2 \\ -\beta_8 \dot{\theta}^2 q^4 - \beta_9 \dot{\theta}^2 q^2 + \beta_{10} \dot{\theta}^2 q^4 - \beta_{11} \dot{\theta}^2 q^4 + \beta_{12} \dot{\theta} \dot{q} q^2 + \beta_{13} q^2 \dot{q}^2 \end{array} \right\}. \tag{33}$$

By applying the Lagrange’s equation to the system Lagrangian equation (33), the system equations of motion are

$$2[\beta_1 + (\beta_2 - \beta_7 - \beta_9)q^2 + (\beta_{10} - \beta_8 - \beta_{11})q^4]\ddot{\theta} + 4(\beta_2 - \beta_7 - \beta_9)\dot{\theta} \dot{q} + 8(\beta_{10} - \beta_8 - \beta_{11})\dot{\theta} q^3 \dot{q} + \beta_3 \ddot{q} + \beta_{10}(\ddot{q} q^2 + 2\dot{q}^2 q) = \frac{2T}{m_B l^2}, \tag{34}$$

$$2[\beta_4 + \beta_{13}q^2]\ddot{q} + [\beta_3 + \beta_{12}q^2]\ddot{\theta} + 2[\beta^2 \beta_5 + (\beta_7 + \beta_9 - \beta_2)\dot{\theta}^2]q + 4[\beta^2 \beta_6 + (\beta_8 - \beta_{10} + \beta_{11})\dot{\theta}^2]q^3 + 2\beta_{13}q\dot{q}^2 = 0. \tag{35}$$

Now four models are produced to describe the problem of rotating beam. The models are the consistent model (CM) where no provision was considered to account for the axial shortening, the potential energy model (PM) that considers the added potential energy due to centrifugal forces and axial shoretning, the kinetic energy model (KM) that considers the axial shortening as time variable and substituted for in the velocity vector and finally the combined potential and kinetic energy model (KPM) that considers both approaches. Each of these models have produced two coupled equations of motion that have some common terms. To produce a generalized model for all models the system of equation is re-written as follows:

$$\begin{bmatrix} 2\{\beta_1 + (\beta_2 - \beta_7 - \beta_9)q^2 + (\beta_{10} - \beta_{11} - \beta_8)q^4\} & \beta_3 - \beta_{12}q^2 \\ \beta_3 + \beta_{12}q^2 & 2(\beta_4 + \beta_{13}q^2) \end{bmatrix} \begin{Bmatrix} \ddot{\theta} \\ \ddot{q} \end{Bmatrix} + \begin{Bmatrix} 4(\beta_2 - \beta_7 - \beta_9)\dot{\theta} q \dot{q} + 8(\beta_{10} - \beta_8 - \beta_{11})\dot{\theta} q^3 \dot{q} + 2\beta_{12}q\dot{q}^2 \\ 2(\beta^2 \beta_5 + (\beta_7 + \beta_9 - \beta_2)\dot{\theta}^2)q + 4(\beta^2 \beta_6 + (\beta_8 + \beta_{11} - \beta_{10})\dot{\theta}^2)q^3 + 2\beta_{13}q\dot{q}^2 \end{Bmatrix} = \begin{Bmatrix} \frac{2T}{m_B l^2} \\ 0 \end{Bmatrix}, \tag{36}$$

where for the corresponding coefficients that vanish for each model are organized in Table 1.

Table 1
Generalized model coefferents

Model	Vanishing coefficients
CM	$\beta_6 \dots \beta_{13} = 0$
PM	$\beta_9 \dots \beta_{13} = 0$
KM	$\beta_7 = \beta_8 = 0$
KPM	None

Table 2
Beam–hub properties

Property	Value
Beam length, L	0.4 m
Beam flexural rigidity, EI	75 N m ²
Beam mass per unit length, ρ	1.35 kg/m
Hub radius, R_H	0.05 m
Hub mass, M_H	3.18 kg

3. Results and discussion

The developed mathematical models describe the dynamics of the rotating beam under the effect of externally applied torque. Different methods used to account for the axial shortening were shown in the previous section to produce different mathematical models that govern the dynamic behaviour of the system. This dynamic behaviour can be quantified by studying the (1) system nonlinear natural frequencies as related to the rotating speed, (2) system coupled dynamic response, (3) sensitivity of the system to the order of deformation and nonlinearity, and (4) system frequency response. In the following subsections each of the above aspects of the dynamic behavior is investigated using as the base parameters data given in Table 2.

3.1. Numerical solutions of the equations of motion

The generalized model of the rotating flexible arm is simulated by applying an actuation torque that rotates the system to a pre-set rotating speed. As a result the beam vibrated at its own natural frequency after the period of torque vanishing. The cascaded frequency spectra for the four different models, CM, PM, KM and KPM are shown in Figs. 3–6, respectively. From Fig. 3, one can observe that increasing the rotating speed decreases the natural frequency and increases the vibration amplitude that can be referred to reducing the beam stiffness as can be justified by Eq. (10). From Eq. (10) one can calculate a critical rotating speed at which the stiffness goes to zero, thus the beam enters into what is known as static instability. When the potential energy is augmented by the axial shortening potential energy, defined previously as the PM, the beam vibration frequencies change with the rotating speed as can be seen in Fig. 4. The vibration frequency increases with the rotating speed accompanied by reduction in the vibration amplitude. The behaviour was previously reported by other investigations and known as the stiffening effect. Similar behaviour can be observed for the KM and KPM models as shown in Figs. 5 and 6, respectively, but with different rates of increase in the vibration frequency and different rates of decrease in the vibration amplitude. In all previous simulations the dynamics of each of the models is obtained naturally as all the nonlinear terms whenever applicable are considered in the models. The difference in the rates of increase in the vibration frequencies and decrease in the vibration amplitude as the rotating speed is increased can be simply related to the existence of these nonlinear terms. However, the way each of the models behaves cannot be assessed by these dynamic simulations and extra tests should be conducted. These tests are finding the natural frequencies as functions of both rotating speed and vibration amplitude.

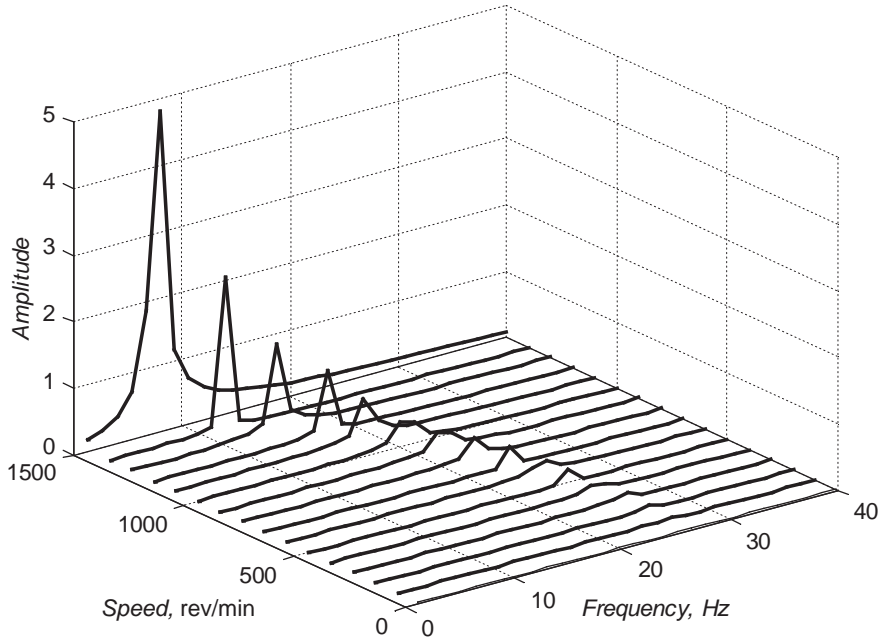


Fig. 3. Cascaded frequency spectrum for the (CM).

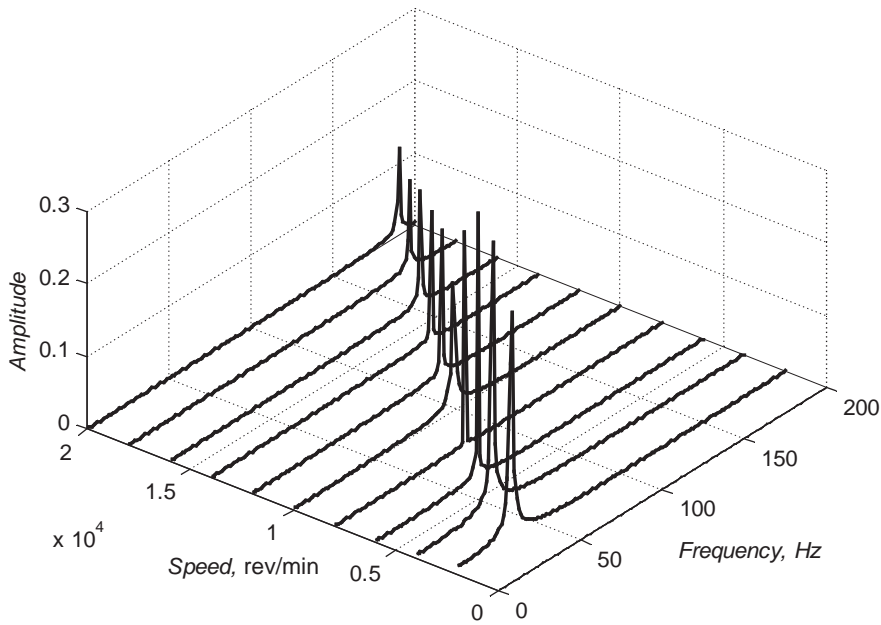


Fig. 4. Cascaded frequency spectrum for the (PM).

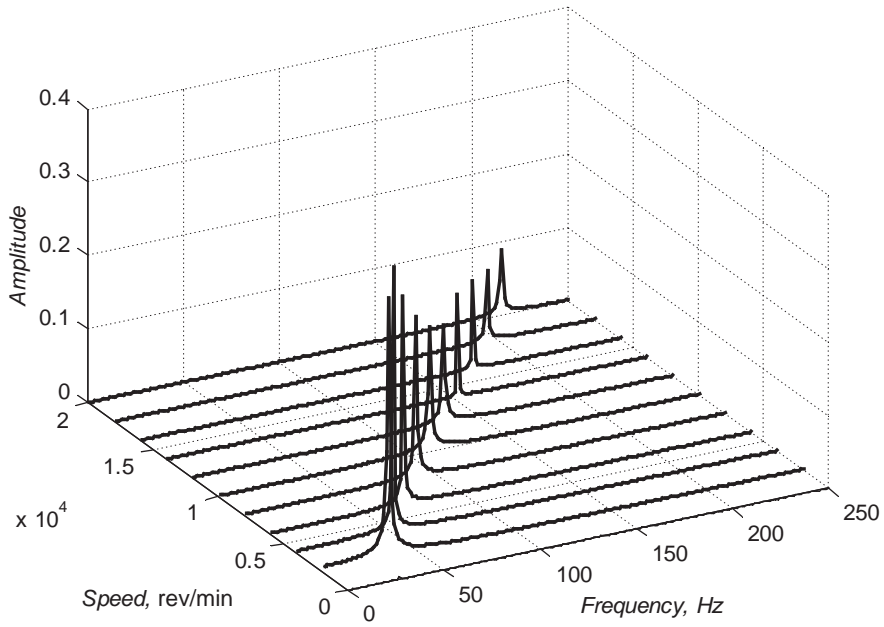


Fig. 5. Cascaded frequency spectrum for the (KM).

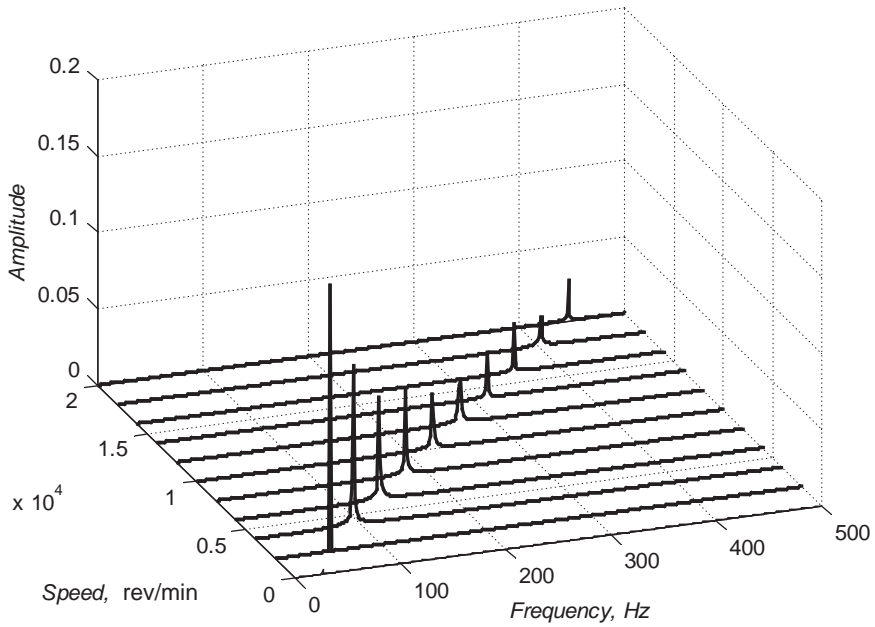


Fig. 6. Cascaded frequency spectrum for the KPM.

3.2. Nonlinear natural frequencies

Due to beam rotation and imposing the stiffening effect the resulting models are non-linear ones, wherein the stiffness and inertia properties are displacement and velocity dependent. To examine these models, their non-linear natural frequencies behavior as related to amplitude of modal deflection is investigated.

To find the rotating beam natural frequencies, the models of Eq. (36), are reduced by assuming that the rotational speed $\dot{\theta}$, is constant. As a result the system is reduced to one differential equation that can be written in the following form:

$$2\beta_4\ddot{q} + 2\beta_{13}[\ddot{q}q^2 + q\dot{q}^2] + 2\beta^2\beta_5q + 4\beta^2\beta_6q^3 + [(\beta_7 + \beta_9 - \beta_2)\dot{\theta}^2]q + 4[(\beta_8 - \beta_{10} + \beta_{11})\dot{\theta}^2]q^3 = 0. \tag{37}$$

It is to be noted that some of the coefficients β_i in Eq. (37) vanishes based on the model used for finding the natural frequencies. Table 1 can be consulted to find out the corresponding vanishing

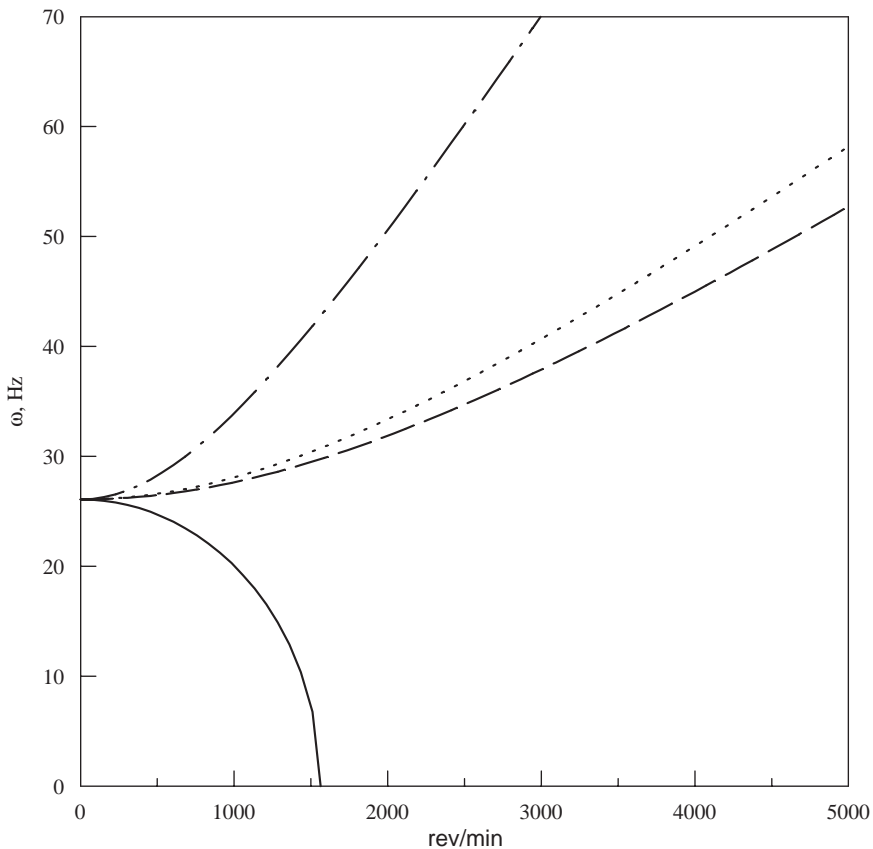


Fig. 7. Nonlinear natural frequency versus rotational speed of the first mode. —, CM; ----, PM; ·····, KM; -·-·-·-·, KPM.

terms in Eq. (37). For convenience, Eq. (37) can be scaled and converted to the dimensionless form

$$q'' + q - \varepsilon_1 \Omega^2 q - \varepsilon_2 \Omega^2 q^3 + \varepsilon_3 (q^2 \ddot{q} + q \dot{q}^2) + \varepsilon_4 q^3 = 0. \tag{38}$$

The prime denotes a derivative with respect to the non-dimensional time $t^* = (\beta^2 \beta_5 / \beta_4)^{1/2} t$, q is the dimensionless tip displacement, $\Omega = \dot{\theta} / \omega_{ni}$ is the dimensionless hub speed ratio, ω_{ni} is the linear natural frequency of the corresponding non-rotating cantilevered beam, and the new coefficients are defined as functions of β s by the following expressions:

$$\varepsilon_1 = \frac{\beta_2 - \beta_7 - \beta_9}{\beta_4}, \quad \varepsilon_2 = \frac{2(\beta_{10} - \beta_8 - \beta_{11})}{\beta_4}, \quad \varepsilon_3 = \frac{\beta_{13}}{\beta_4}, \quad \varepsilon_4 = \frac{2\beta_6}{\beta_5} \tag{39}$$

Following closely the analysis of Ref. [14] of using the method of time transformation, the nonlinear natural frequencies of the four models (CM, PM, KM, KPM) are found as a function of rotating speed for the first three modes. As a requirement of the method of time transformation the vibration amplitude should be defined. The amplitudes used in the present calculations are

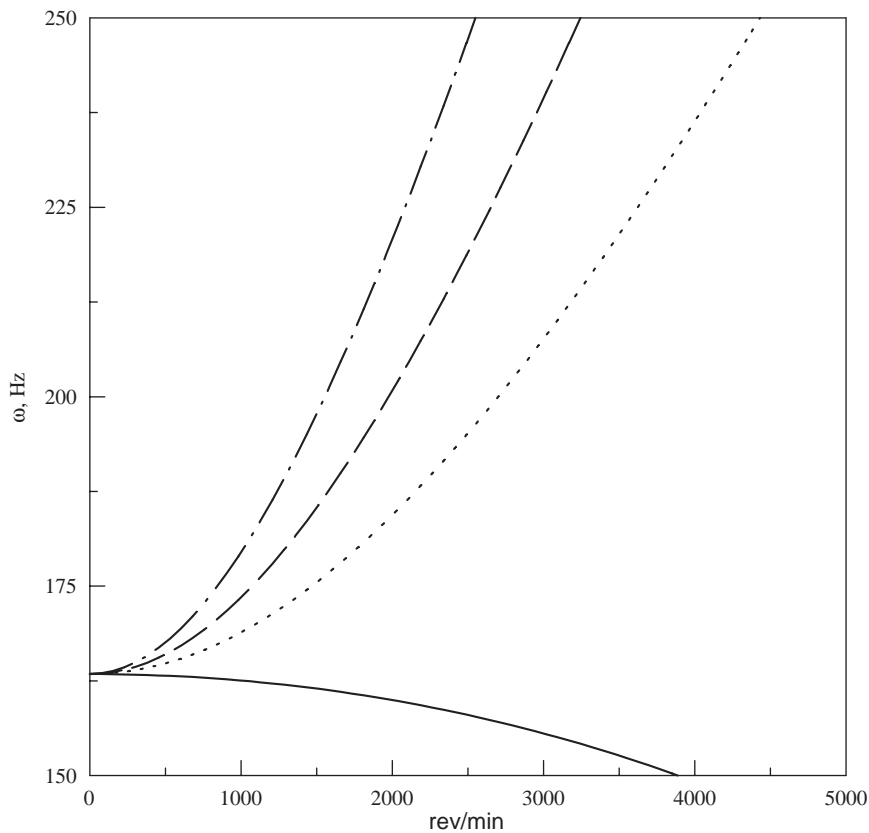


Fig. 8. Nonlinear natural frequency versus rotational speed of the second mode ———, CM; -----, PM; ·······, KM; —·—·—·, KPM.

those obtained from the previous dynamic simulations. The nonlinear natural frequency of the first mode for the four models is presented in Fig. 7. As shown the CM model natural frequency decreases with the rotating speed until it crosses the speed axis which agrees with the previous simulations. The PM, KM and KPM models show that the natural frequency increases with rotating speed, but at different rates. The highest rate is the one given by KPM model. The second and third modes natural frequencies show similar behaviour but with a hardening rate higher in the PM model than the KM model, Figs. 8 and 9.

To investigate the role of each of the models when the system nonlinearities is considered, the natural frequencies at selected running speeds are calculated as a function of the tip deflection amplitude. For this analysis only the three nonlinear models are considered as the consistent model is a linear one. At dimensionless running speed $\Omega = 1$, the natural frequencies of the three models as a function of tip deflection non-dimensional amplitude are presented in Fig. 10, for the first bending mode. One can observe that the KM gives hardening with amplitude increase linearly with very small slope that can be taken as constant. In contrast the PM model shows hardening behaviour with the amplitude that almost follows the cubic curve as shown in Fig. 10. The KPM

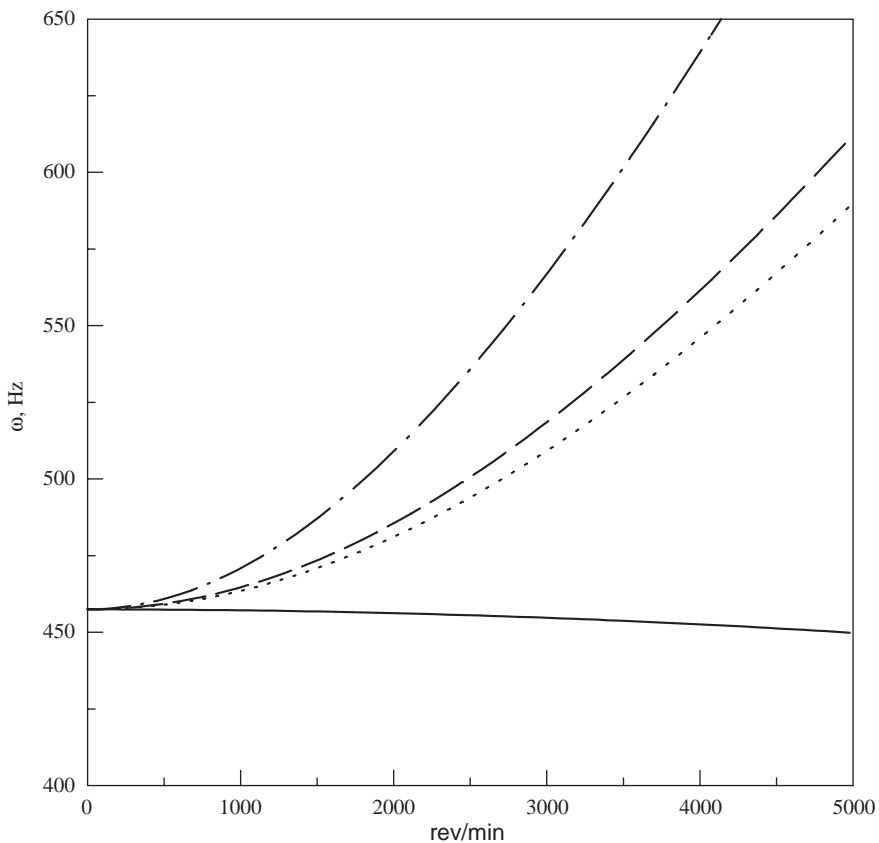


Fig. 9. Nonlinear natural frequency versus rotational speed of the third mode ———, CM; -----, PM; ·······, KM; —·—·—·, KPM.

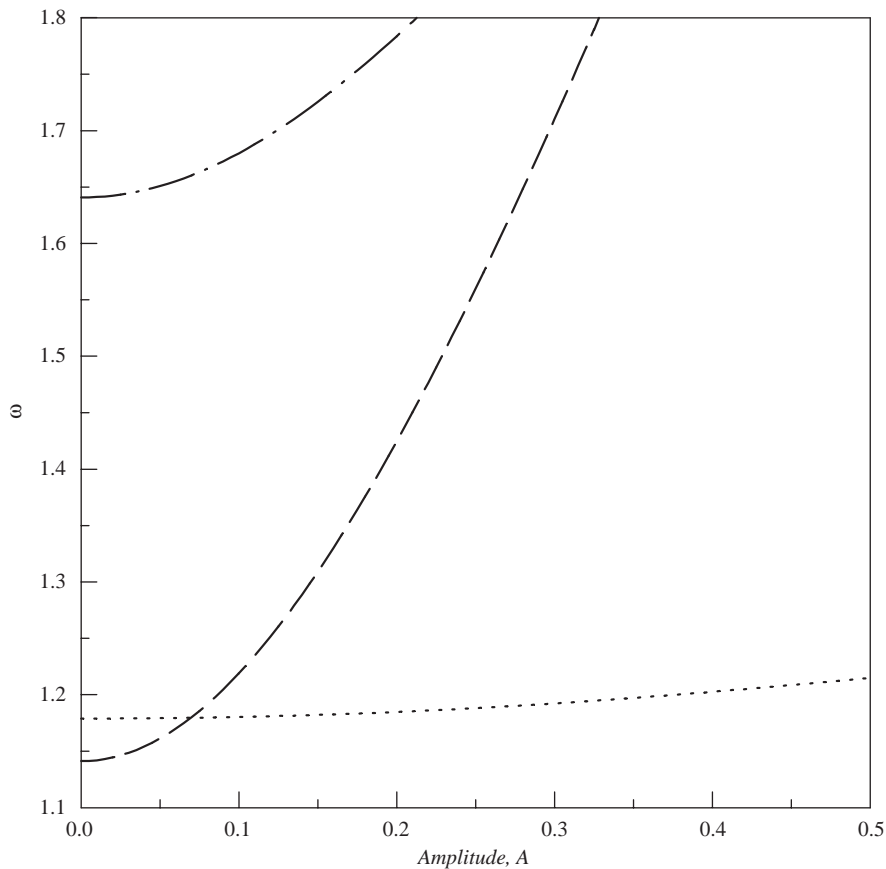


Fig. 10. Dimensionless nonlinear natural frequency versus the amplitude of the first mode, $\Omega = 1$; -----, PM; ·······, KM; — · — · — ·, KPM.

model shows hardening with increase in amplitude that can be described as a second order. Moreover, one can observe that PM and KM models intersect at an amplitude of 0.07 that means both predict the same natural frequency only at this amplitude. For amplitudes lower than 0.07, PM predicts lower natural frequencies. At very low amplitudes, the KPM model predicts the natural frequency almost 60% higher than both models. The common feature of all three models for the first mode is that they produced hardening effect with the vibration amplitude. The second mode nonlinear natural frequency predictions using the PM, KM and KPM models are shown in Fig. 11 as a function of the amplitude. The PM and KPM models give hardening behaviour while the KM gives softening behaviour as function of amplitude. The third mode natural frequencies predictions of the three models are shown in Fig. 12. The PM model still gives hardening behaviour while the KM and KPM models show softening behaviour. This means that the amount of softening imposed by the KM model overcomes the hardening effect of the PM model when both are used simultaneously. The natural frequencies as a function of the vibration

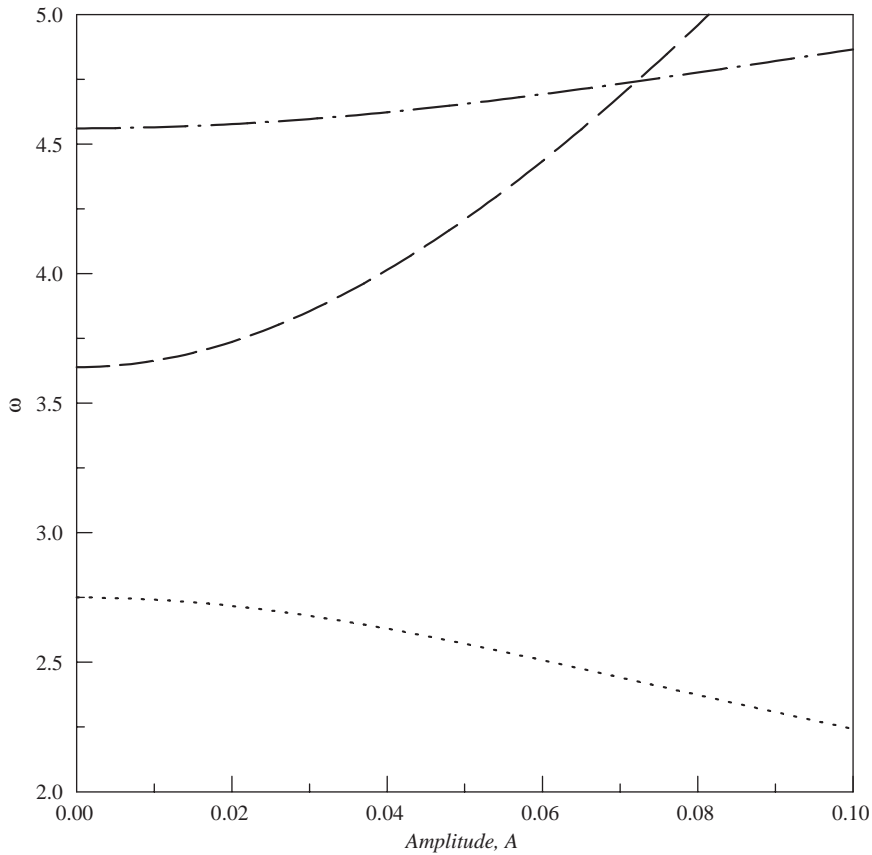


Fig. 11. Dimensionless nonlinear natural frequency versus the amplitude of the second mode, $\Omega = 1$; -----, PM; ·······, KM; —·—·—·, KPM.

amplitudes were also calculated for higher rotating speeds with similar predictions obtained as in Figs. 10–12. The main finding of the natural frequencies predictions as a function of the vibration amplitude is the softening behaviour that appeared at the KM. This behaviour is critical as naturally one expects the rotating beams to harden as a result of rotation and at the same time a concern arises as to the correctness of the KM model in dealing with rotating structures.

3.3. Frequency response analysis

The generalized model can be excited by an external harmonic force $F \sin \omega_e t^*$, however the running speed Ω is kept constant, as can be represented by the following equation:

$$q'' + q - \varepsilon_1 \Omega^2 q - \varepsilon_2 \Omega^2 q^3 + \varepsilon_3 (q^2 \ddot{q} + q \dot{q}^2) + \varepsilon_4 q^3 = F \sin \omega_e t^*, \tag{40}$$

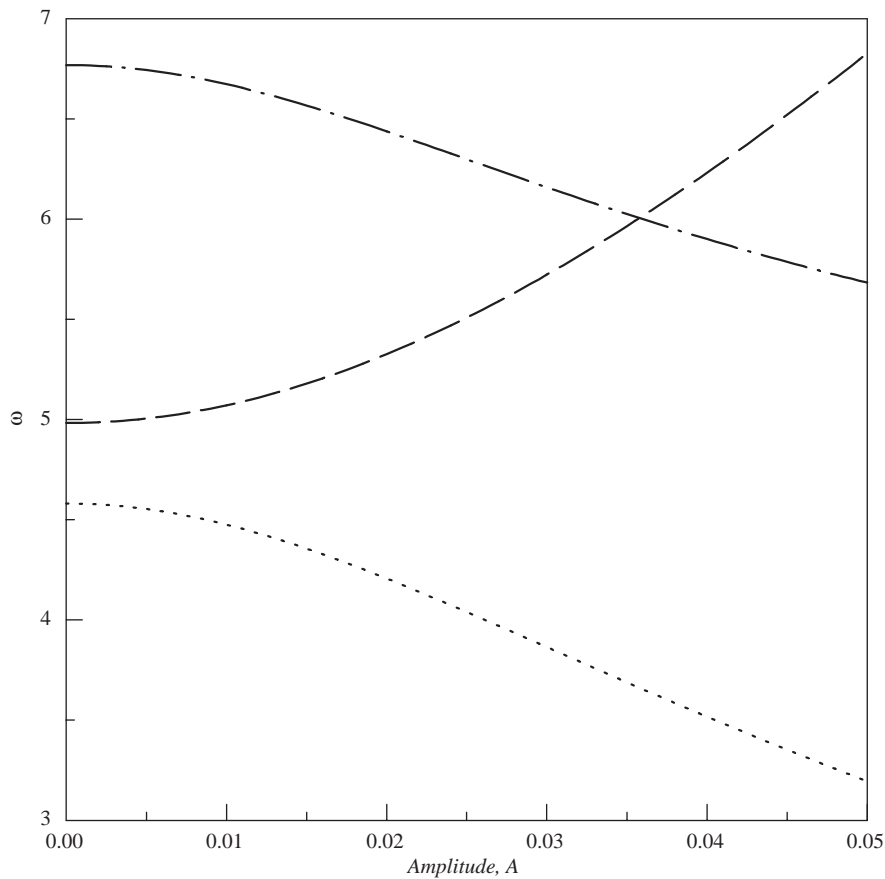


Fig. 12. Dimensionless nonlinear natural frequency versus the amplitude of the third mode, $\Omega = 1$; -----, PM; , KM; — · — · — · , KPM.

where F is a small excitation amplitude and ω_e is the dimensionless external excitation frequency.

To find the frequency response, the method of harmonic balance is used for the three models. The frequency response of the first mode is shown in Fig. 13, wherein the PM model shows clear hardening and the KM and KPM show small hardening with the amplitude. Moreover, one can observe that an equivalent backbone curve starts at 1.65 times the linear resonance frequency. The second frequency response is shown in Fig. 14, in which the PM model keeps reflecting the hardening behaviour and the KM and KPM give softening behaviour. This contradicts the behaviour shown in the natural frequencies prediction of Fig. 10 that showed softening for the KM and hardening for the KPM. The third mode frequency response is shown in Fig. 15 for the three models. Similar behaviour can be seen as that for the second mode.

To this end one can observe that the three models give different predictions for the natural frequencies and for the frequency response behaviour. The major finding is that the PM model

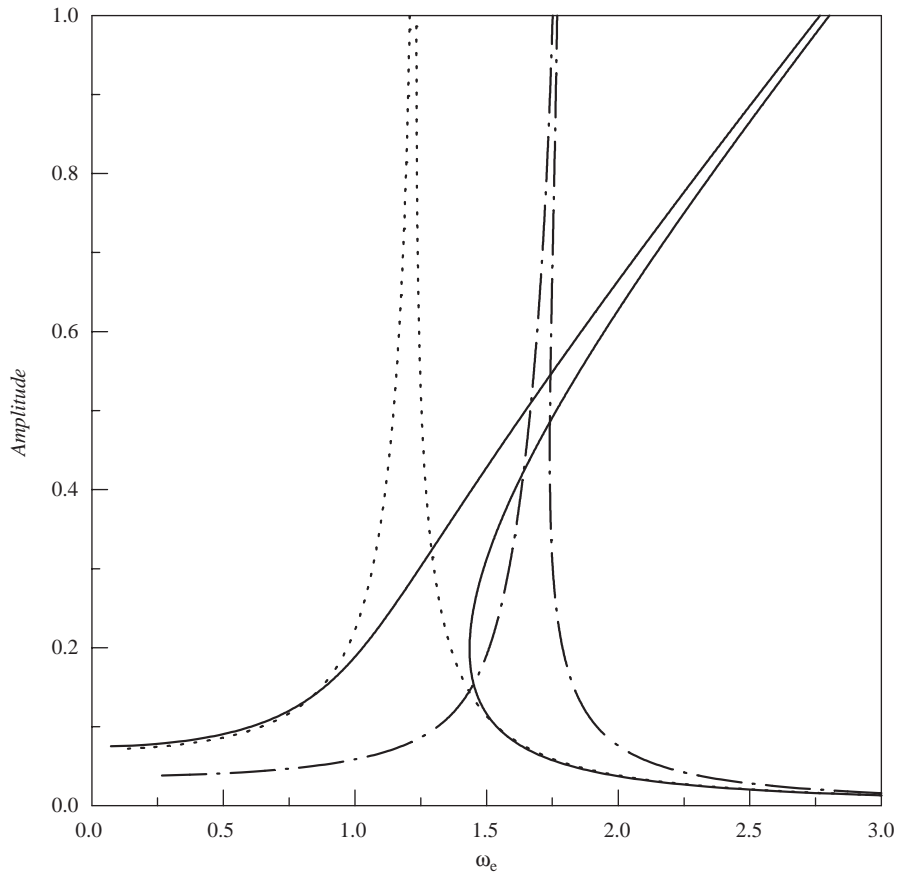


Fig. 13. Frequency response versus the excitation frequency for the first mode, $\Omega = 1$; -----, PM; ·······, KM; —·—·—·, KPM.

showed consistent predictions in all three analysis approaches and the KM and KPM showed contradictions based on the method used. This gives more confidence in the PM method for accounting for the effect of rotation on the beam dynamic behaviour and puts doubts on using the KM model or what is known as the inextensibility condition. When the KPM model is used which is combining both methods one can see that it predicts the natural frequency and frequency response by about 65% higher than the linear model for small amplitudes. This indicates that using the KPM model should be excluded from the approaches.

4. Conclusions

The problem of rotating beam shortening is studied in this paper. The available three methods for accounting for the beam shortening are considered and a generalized model is developed. The

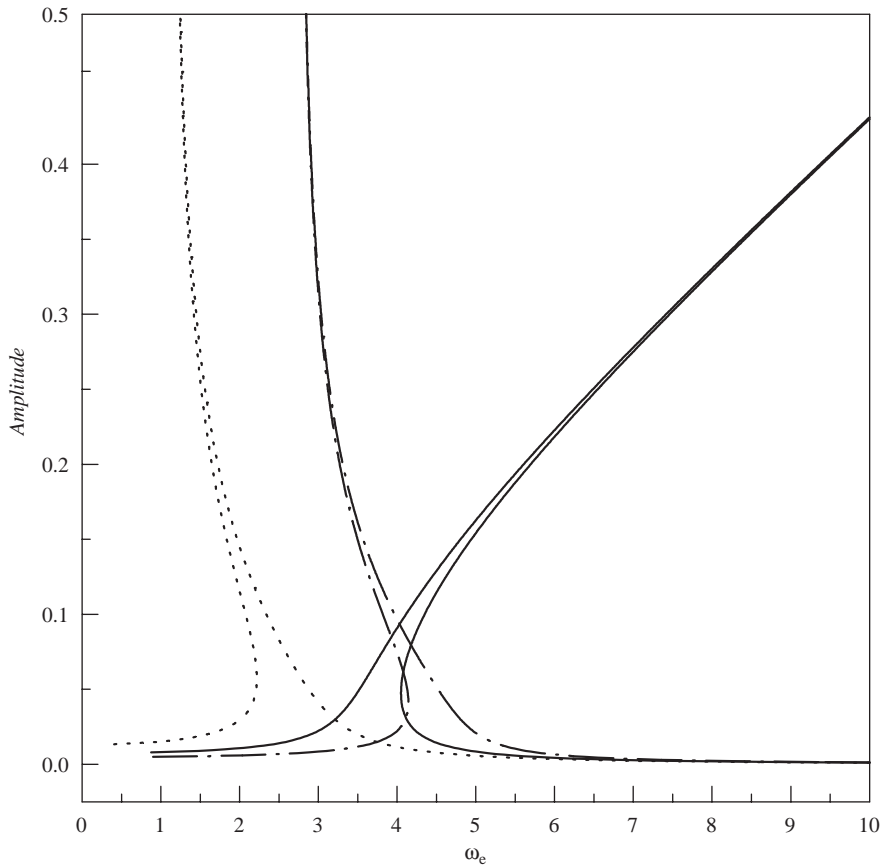


Fig. 14. Frequency response versus the excitation frequency for the second mode, $\Omega = 1$; -----, PM; ·······, KM; —·—·—·—, KPM.

model was analysed using the time integration for the beam that is rotated to a target speed and the frequency spectrums were analysed. The consistent model that takes no care of the effect of rotation shows that the beam can be rotated only to its first natural frequency after which the beam goes to static instability that enforces the need for using a method to reflect the actual dynamic behaviour. The PM, KM, and KPM methods are used to produce different models that are consequently analysed using the dynamic simulations, the nonlinear natural frequency analysis and the harmonic balance frequency response. The results of analysis showed that the consistent approach that handles both the effect of rotating speed and the effect of vibration amplitude for all modes correctly is the PM model. The KM model reflected softening behaviour that cannot be accepted physically by rotating structures for higher modes. Moreover, the combined KPM method showed incorrectness at low amplitudes that contradicts the linear theory. To give more rigid conclusions in this direction an experimental study is highly recommended, although the complexity of the experiments is expected.

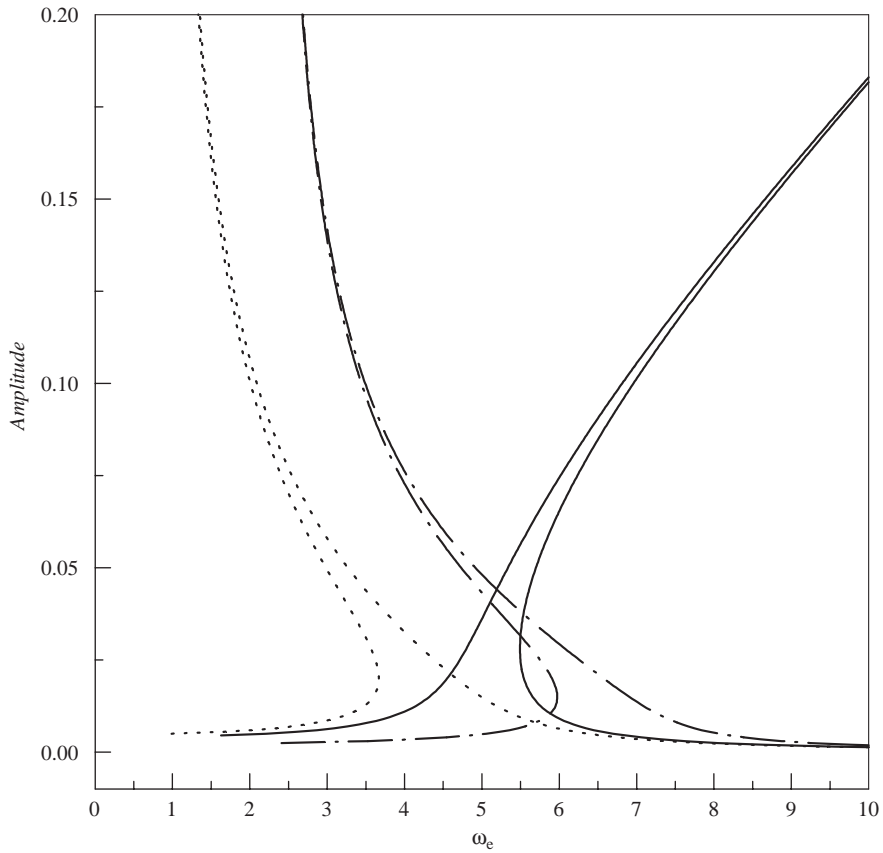


Fig. 15. Frequency response versus the excitation frequency for the third mode, $\Omega = 1$; -----, PM; $\cdots\cdots\cdots$, KM; ————, KPM.

Acknowledgement

The authors acknowledge the support of the University of Jordan. The second author acknowledges the endless support of King Fahad University of Petroleum and Minerals.

References

- [1] S.V. Hoa, Vibration of a rotating beam with tip mass, *Journal of Sound and Vibration* 67 (1979) 369–381.
- [2] T.R. Kane, R.R. Ryan, A.K. Banerjee, Dynamics of a cantilever beam attached to a moving base, *Journal of Guidance* 10 (1987) 139–151.
- [3] H. Baruh, S.K. Tadikonda, Issues in the dynamics and control of flexible robot manipulators, *Journal of Guidance* 12 (1989) 659–671.
- [4] H.P. Lee, Vibration on an inclined rotating cantilever beam with tip mass, *Journal of Vibration and Acoustics* 115 (1993) 241–245.

- [5] S. Mulmule, G. Singh, R. Venkateswara, Flexural vibrations of rotating tapered timoshenko beams, *Journal of Sound and Vibration* 160 (1993) 372–377.
- [6] S.K. Tadikonda, H.T. Chang, On the geometric stiffness in flexible multibody dynamics, *Journal of Vibrations and Acoustics* 117 (1995) 452–461.
- [7] B.O. Al-Bedoor, Dynamic model of coupled shaft torsional and blade bending deformations in rotors, *Computer Methods in Applied Mechanics and Engineering* 169 (1999) 177–190.
- [8] B.O. Al-Bedoor, Reduced-order nonlinear model dynamic model of coupled shaft-torsional and blade-bending vibrations in rotors, *Journal of Engineering for Gas Turbines and Power* 123 (2001) 82–88.
- [9] B.O. Al-Bedoor, M.N. Hamdan, Geometrically non-linear dynamic model of a rotating flexible arm, *Journal of Sound and Vibration* 240 (2001) 59–72.
- [10] A.A. Al-Qaisia, Nonlinear free vibration of a rotating beam carrying a tip mass with rotary inertia, *Proceedings of ASME 2002 Pressure Vessels & Piping Conference*, Vol. 447, 2002 pp. 1–8, PVP2002-1510.
- [11] A. A. Al-Qaisia, Nonlinear dynamics of a rotating beam clamped with an attachment angle and carrying an inertia element, *Arabian Journal for Science and Engineering*, in press.
- [12] H. El-Absy, A.A. Shabana, Geometric stiffness and stability of rigid body modes, *Journal of Sound and Vibration* 207 (1997) 465–496.
- [13] H.N. Arafat, A.H. Nayfeh, C. Chin, Nonlinear nonplanar dynamics of parametrically excited cantilever beams, *Nonlinear Dynamics* 15 (1998) 31–61.
- [14] A.A. Al-Qaisia, Effect of fluid mass on non-linear natural frequencies of a rotating beam, in: *Proceedings of ASME 2003 Pressure Vessels & Piping Conference*, Vol. 468 (PVP2003), 2003.